Identify CRNDE and LINC00152 as the key lncRNAs in age-related degeneration of articular cartilage through comprehensive and integrative analysis

Pengfei Hu[1,2,*], Fangfang Sun[3,*], Jisheng Ran[1,2] and Lidong Wu[1,2]

[1] Department of Orthopedic Surgery, the Second Affiliated Hospital, School of Medicine, Zhejiang University, Hangzhou, Zhejiang, China

[2] Orthopedics Research Institute of Zhejiang University, Hangzhou, Zhejiang, China

[3] Key Laboratory of Cancer Prevention and Intervention, China National Ministry of Education, the Second Affiliated Hospital, Cancer Institute, School of Medicine, Zhejiang University, Hangzhou, Zhejiang, China

[*] These authors contributed equally to this work.

ABSTRACT

Background. Osteoarthritis (OA) is one of the most important age-related degenerative diseases, and the leading cause of disability and chronic pain in the aging population. Recent studies have identified several lncRNA-associated functions involved in the development of OA. Because age is a key risk factor for OA, we investigated the differential expression of age-related lncRNAs in each stage of OA.

Methods. Two gene expression profiles were downloaded from the GEO database and differentially expressed genes (DEGs) were identified across each of the different developmental stages of OA. Next, gene ontology (GO) functional and Kyoto Encyclopedia of Genes and Genomes (KEGG) pathway analyses were performed to annotate the function of the DEGs. Finally, a lncRNA-targeted DEG network was used to identify hub-lncRNAs.

Results. A total of 174 age-related DEGs were identified. GO analyses confirmed that age-related degradation was strongly associated with cell adhesion, endodermal cell differentiation and collagen fibril organization. Significantly enriched KEGG pathways associated with these DEGs included the PI3K–Akt signaling pathway, focal adhesion, and ECM–receptor interaction. Further analyses via a protein–protein interaction (PPI) network identified two hub lncRNAs, CRNDE and LINC00152, involved in the process of age-related degeneration of articular cartilage. Our findings suggest that lncRNAs may play active roles in the development of OA. Investigation of the gene expression profiles in different development stages may supply a new target for OA treatment.

Subjects Bioinformatics, Geriatrics, Orthopedics

Keywords Osteoarthritis, CRNDE, LINC00152, KEGG pathway, DEGs, GO annotation

Submitted 29 January 2019
Accepted 24 April 2019
Published 28 May 2019

Corresponding author
Lidong Wu, wulidong@zju.edu.cn

Academic editor
Ugo Bastolla

Additional Information and Declarations can be found on page 15

DOI **10.7717/peerj.7024**

Copyright
2019 Hu et al.

Distributed under
Creative Commons CC-BY 4.0

OPEN ACCESS

INTRODUCTION

Osteoarthritis (OA) is a common chronic joint disease in elderly individuals, with weight-bearing joints such as the knees, hips, and the spine being the most commonly affected.

Between 2011 and 2012, the prevalence of symptomatic knee OA in China was 8.1% (*Tang et al., 2016*). OA progresses slowly over time, eventually resulting in joint pain, stiffness, and dysfunction (*Hunter & Felson, 2006*). With the growing number of patients suffering from OA, the treatment costs of OA are expected to present a huge economic burden to both individuals and health systems worldwide. While the exact mechanisms underlying OA remain poorly understood, numerous risk factors have been identified, including age, obesity, sex, genetic predisposition, and joint injury (*Loeser, 2017*; *Silverwood et al., 2015*). Among these factors, age is one of the most important critical influences on the degeneration of articular cartilage. Previous studies have demonstrated that the prevalence of radiographic knee OA increases with age (*Shane Anderson & Loeser, 2010*). Aging-related changes in joint tissues include accumulation of senescent secretory phenotype cells, increased expressions of catabolic factors, a gradual loss of extracellular cartilage matrix, and oxidative stress (*Campisi & d'Addadi Fagagna, 2007*; *Ding et al., 2005*; *Henrotin, Bruckner & Pujol, 2003*; *Wu et al., 2002*). Moreover, age-related increases in mesenchymal stromal cells in the bone marrow are also thought to regulate of osteoblast formation and bone remodeling (*Ganguly et al., 2017*).

Long non-coding RNAs (lncRNAs), defined as non-coding capacity RNAs >200 bp in length, play an important role in transcriptional regulation (*Ponting, Oliver & Reik, 2009*). Recent studies have identified several lncRNA-associated functions involved in the development of human diseases, including several forms of cancer, cardiovascular disease, diabetes, and osteoporosis (*Cao et al., 2013*; *Hao et al., 2015*; *Huang, 2018*; *Leti & DiStefano, 2017*; *Wang et al., 2018b*), as well as OA. Using DNA microarrays and bioinformatic approaches, Ming et al. identified a number of lncRNAs that are differentially expressed in OA cartilage compared to normal samples (*Fu et al., 2015*). Similarly, Xiang et al. found that synovium samples obtained from OA patients showed differential expression of numerous mRNAs and lncRNAs (*Xiang et al., 2018*). In addition, an increasing number of lncRNAs have been implicated in chondrocytes proliferation and cartilage metabolism. For example, increased expression of lncRNA-ZFAS1 was shown to induce the proliferation and migration of chondrocytes (*Ye et al., 2018*), while increased expression of lncRNA-HOTAIR contributes to chondrocytes apoptosis and matrix degradation (*Hu et al., 2018*). Finally, lncRNA-CIR acts as a sponge for miRNA-27b, resulting in increased extracellular matrix degradation via its effects on MMP13 expression (*Li et al., 2017c*). Taken together, these data suggest that lncRNAs play key roles in the pathogenesis of OA.

Because OA is an age-related chronic disease, morphological and molecular biological characters may appear differently in different stages. Here, to explore differential expression of age-related lncRNAs in each stage of OA, we examined two previously published OA gene datasets available in the Gene Expression Omnibus (GEO) database. Differential expression of lncRNAs across different developmental stages was examined by comprehensive bioinformatic analyses. Then the differentially expressed lncRNAs were correlated with other DEGs and potential diseases based on data obtained from the RAID and MNDR databases. Moreover, Gene Ontology (GO) and Kyoto Encyclopedia of Genes and Genomes (KEGG) pathway enrichment analyses were also performed, and

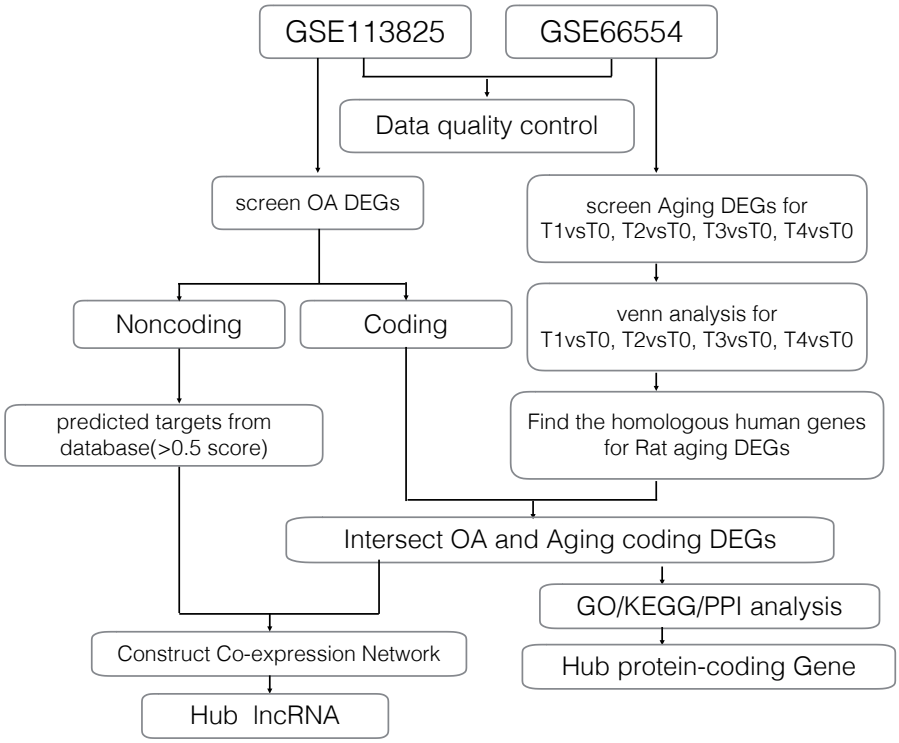

Figure 1 **Workflow of the bioinformatics analyses.**
Full-size DOI: 10.7717/peerj.7024/fig-1

a protein–protein interaction (PPI) network was used to screen for crucial genes and lncRNAs.

MATERIALS AND METHODS

Expression profile dataset

Gene expression profiles for age-related degeneration in rat knee articular cartilage at different development stages (GSE66554) were obtained from the GEO database and analyzed alongside a second gene expression dataset (GSE113825) which investigated lncRNA and mRNA expression profiles of human knee OA. A detailed workflow of the data analyses is shown in Fig. 1. The quality of gene expression data was analyzed and visualized using the ggplot2 package of R software for each sample.

Differential gene expression analyses

In GSE66554, the authors grouped rats as newborn (T0), youth (T1), adult (T2), early-stage elderly (T3), and later-stage elderly (T4). To identify age-related DEGs, we compared the different stages of rats with T0. We also identify DEGs between RNA-seq data of normal human cartilage samples and OA samples in GSE113825. The Linear Models for Microarray data (LIMMA) (limma) package, which includes lmFit, eBayes, and topTable functions, was used for pairwise comparison of DEGs (*Ritchie et al., 2015*). $P < 0.05$ and abs($\log_2$)fold change (FC) >1 were used as the cut-off criteria.

GO annotation and KEGG pathway enrichment analyses of DEGs

The R package bioMart was used to transform rats genes into homologous human genes. Then we narrowed down the protein coding DEGs by calculating intersection between these homologous human genes and OA DEGs (from GSE113825) to identify age-related OA DEGs. GO annotation, a classic method used to describe subcellular location, molecular function, and the biological attributes of DEGs, was applied (*Ashburner et al., 2000*). KEGG, a collection of databases summarizing genomes, biological pathways, and health information, was used to clarify the potential role of the DEGs (*Kanehisa & Goto, 2000*). GO functional analyses encompassing biological processes (BP), cell components (CC), and molecular functions (MF) was performed using the Database for Annotation, Visualization and Integrated Discovery (DAVID; ver. 6.8), with $P < 0.05$ used as a cutoff.

PPI network construction and hub gene identification

The Search Tool for the Retrieval of Interacting Genes (STRING, http://string-db.org) was used to create a PPI network for the DEGs (*Szklarczyk et al., 2015*), which was visualized using Cytoscape (ver. 3.5.1). Genes served as "nodes" in the PPI network and the line segment between two nodes represented associated interactions. The color of the lines between genes indicates the degree of the interaction. The centiscape plugin was used to determine the degree of connectivity for each node in the PPI network. Genes with a degree >5 were defined as hub genes. The differentially expressed lncRNA-mRNA interaction network was built and displayed using Cytoscape. lncRNAs interacting with the greatest number of hub genes (mRNA) in the network were defined as hub lncRNAs.

Patient samples preparation and qRT-PCR validation

This study was approved by the Ethics Committee of the 2nd Affiliated Hospital, School of medicine, Zhejiang University, Hangzhou, China (No.2018-043) and written informed consent was obtained for each participant. Femoral heads were collected from eight osteoarthritis patients and eight femoral neck fracture patients who underwent total hip arthroplasty. Then the cartilages obtained from the femoral head (nearly 1 cm*1 cm) were preserved in liquid nitrogen until use. Total RNA was extracted using TRIzol reagent (Thermo Fisher Scientific, Inc., Waltham, MA, USA) according to the manufacturer's instructions. And 1μg RNA was reverse-transcribed using the cDNA synthesis kit (Thermo Fisher Scientific, Inc., Waltham, MA, USA). RT-PCR was performed using the SYBR Premix Ex Taq II (Takara Biotechnology, Dalian, China) system on the following steps: 45 cycles of 95 ° C for 15 s and 60 ° C for 30 s. The sequences of the primers used in the reaction are listed in Table 1. Relative gene expression was calculated using the $2^{-\Delta\Delta Ct}$ method. 18S served as the internal control gene.

Statistical analysis

All data are presented as means ± standard deviation (SD). All experiments were performed at least three times. Student's t-test was performed using SPSS (ver. 19.0; IBM Corp., Armonk, NY, USA) and GraphPad Prism 7 (GraphPad Software Inc., La Jolla, CA, USA) software. For all analyses, a p value <0.05 was considered to indicate statistical significance.

Table 1 Real-Time PCR Primers.

ID	Primer Sequences(5′to 3′)
CRNDE	CTCTAGTCGTGTCCCCTCGT
	CTAGCCCACGGGACGTCTG
LINC00152	TGGCACAGTCTTTTCTCTACTCA
	GTCAAGAGGTTTCCAGGGGC
18S	CCTGAGAAACGGCTACCACA
	ACCAGACTTGCCCTCCAATG

RESULTS

Data distribution analyses and DEG screening

In GSE113825, a total of 95,722 genes were detected in each sample. The expression values (ranging from 0 to 20 $\log_2$ [fragments per kilobase of transcript, per million fragments sequenced, FPKM]) and the distributions were similar between normal group and OA group (Fig. 2A). Principal component and h-cluster analyses showed that samples were easily grouped into different groups. As for GSE66554, a total of 36685 genes were detected in each sample, with the values and distributions of these genes similar across the five groups (Fig. 2B). Based on these assessments, further bioinformatics analyses could be performed based on the available data.

Following data processing using limma, we identified 4470 DEGs (1658 upregulated, 2812 downregulated) in human normal vs. OA, including 2891 DEGs (1596 upregulated, 1295 downregulated) in rat T0 vs. rat T1, 4354 DEGs (2451 upregulated, 1903 downregulated) in rat T0 vs. rat T2, 5606 DEGs (2703 upregulated, 2903 downregulated) in rat T0 vs. rat T3, and 14063 DEGs (6432 upregulated, 7631 downregulated) in rat T0 vs. rat T4 (Fig. 2C).

Intersection between the predicted targets of lncRNAs and DEGs

Using the GSE66554 rat OA dataset, we identified a total of 1355 DEGs common across each of the different stages (Fig. 3A). Hierarchical clustering of the identified DEGs is displayed as a heatmap in Fig. 3B. Next, homologous human genes were identified for each of the rat DEGs and compared against DEGs identified in the human OA dataset (Fig. 3C), resulting in an overlap of 174 age-related OA genes, including 33 upregulated and 141 downregulated genes (Table S1). Alignment of these to the human genome is shown in Fig. 3D, as intuitively, green means go and red means stop/downregulated.

GO annotation and KEGG pathway enrichment analyses

GO annotation and KEGG pathway enrichment analyses were performed to better understand the functional significance of the DEGs. Biological processes (BP) were significantly enriched for cell adhesion, endodermal cell differentiation, collagen fibril organization, regulation of cell migration, and cell–matrix adhesion (Fig. 4A). Significant cellular component (CC) terms revealed enrichment in extracellular exosome, extracellular space, proteinaceous extracellular matrix, focal adhesion, and sarcolemma. Finally, the top five molecular functions (MF) identified were calcium ion binding, extracellular matrix

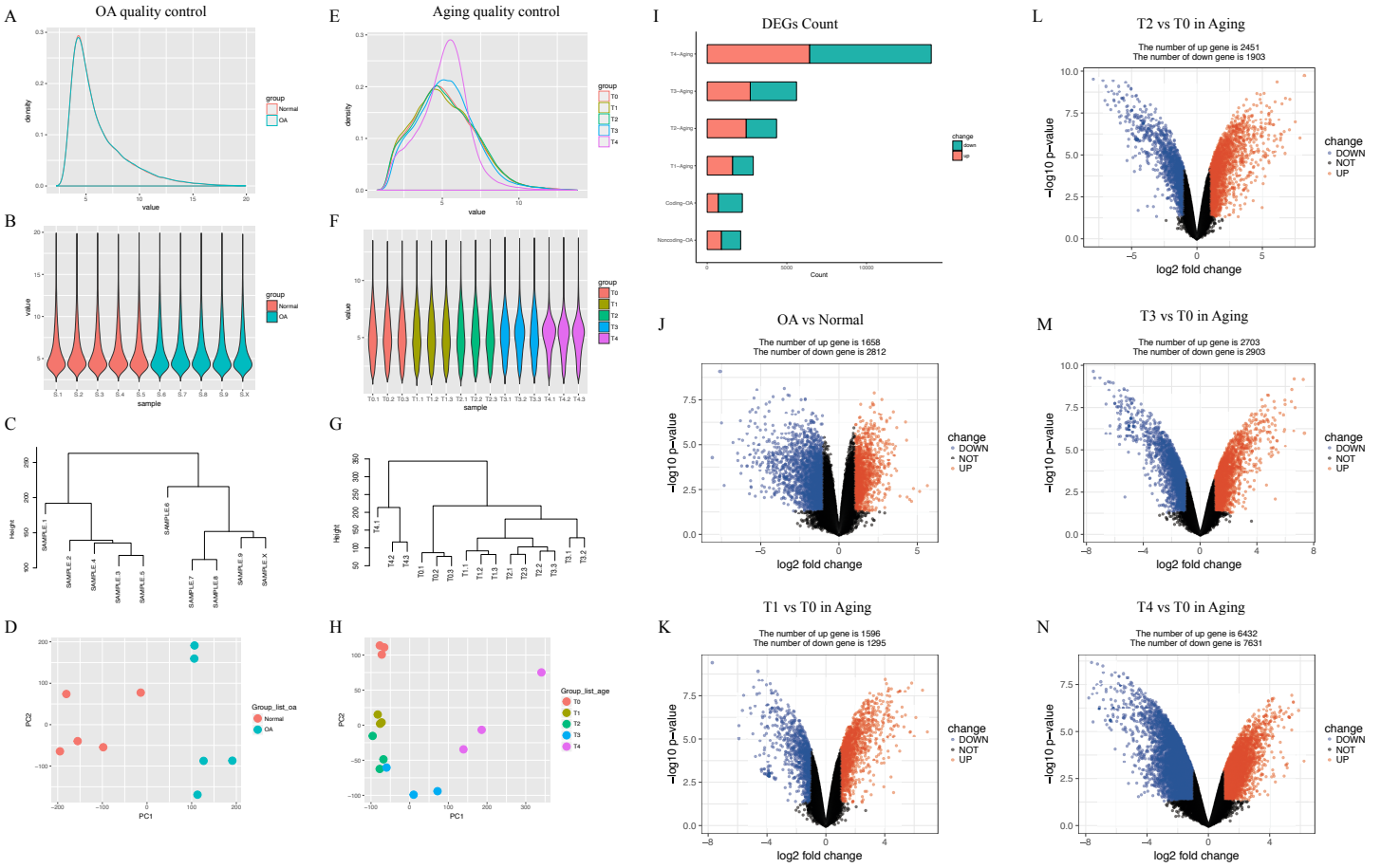

Figure 2 Distribution analyses of gene expression. (A) Distribution of gene expression levels in GSE113825. The x-axis indicates the $\log_2$ value (fragments per kilobase of transcript, per million fragments sequenced [FPKM]) and the y-axis shows the proportion of genes. (B) Distribution of genes expression for each sample in GSE113825. Individual samples are shown on the x-axis, with gene value distribution plotted on the y-axis. (C) Cluster analyses for all samples in GSE113825. (D) Principle component analyses of two groups in GSE113825, plotted as the first and second principal components. Dots represent the principal component value of each sample. (E–H) Represent the distribution analyses for GSE66554. (I) Number of differentially expressed genes (DEGs) identified in each group. (J–N) Volcano plots displaying pairs of expressed genes, where the x- and y-axis represent the log-transformed threshold values. Red dots indicate all significantly upregulated genes and blue dots indicate all significantly downregulated genes that passed the screening threshold. Black dots represent nonsignificant genes.

Full-size DOI: 10.7717/peerj.7024/fig-2

structural constituent, semaphorin receptor binding, chemorepellent activity, and spectrin binding. All significantly enriched entries are shown in a histogram in Fig. 4B. KEGG analyses of the DEGs revealed enrichment for 18 terms (Fig. 4C). The top five significantly enriched KEGG pathways were the PI3K–Akt signaling pathway, focal adhesion, ECM–receptor interaction, protein digestion and absorption, and pathways in cancer. Detailed information regarding each of the DEGs involved in the BP analyses and KEGG pathway are listed in Fig. 4.

PPI network construction and hub lncRNAs identification

We constructed a putative PPI network map for the overlapping DEGs using the STRING database, which was visualized with Cytoscape. Excluding the DEGs distributed on the

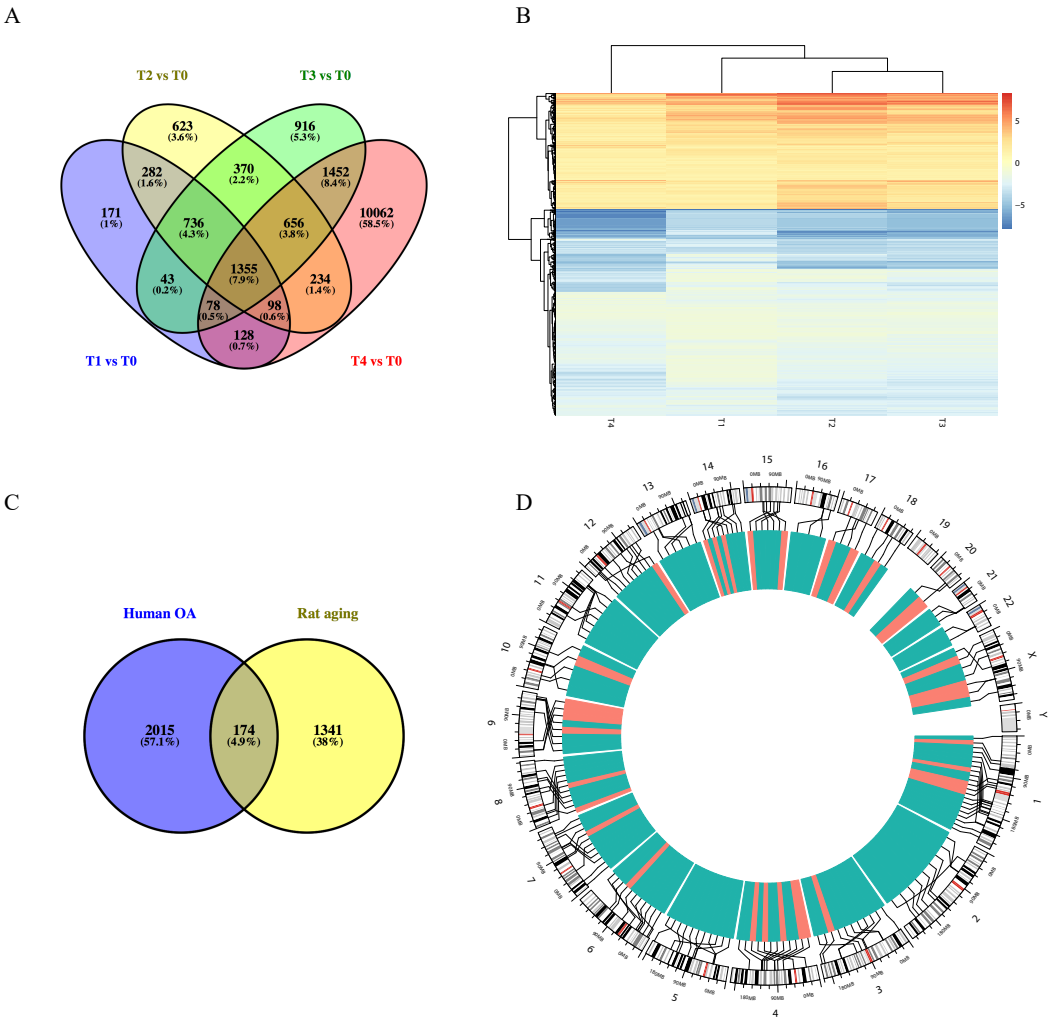

Figure 3 Functional analyses of differentially expressed long non-coding RNA (lncRNA)-targeted DEGs. (A) Venn diagram of DEGs across different growth stages in GSE66554. (B) Hierarchical clustering analyses of DEGs common to all four groups. (C) Venn diagram demonstrating the overlap between the OA aging groups. A total of 174 DEGs were identified as age-related genes, including 33 upregulated and 141 downregulated genes. (D) Circle graph showing the detailed location of 174 DEGs across the human genome. Chromosome locations are marked by lines, upregulated genes shown in red and downregulated genes shown in green. Chromosomes 1, 13, and 4 were most common locations for age-related DEGs in OA.

Full-size DOI: 10.7717/peerj.7024/fig-3

edge of the PPI network, the remaining 110 central DEGs were evaluated using the centiscape plugin. After degree calculation, a total of 34 hub genes were colored red in the PPI network (Fig. 5A and Table 2). Using this same approach, we also constructed a lncRNA–gene co-expression network. Each hub lncRNA was determined by calculating its downstream hub genes whose count should be ranked in the top three (minimum of two genes). A total of 23 lncRNAs were screened and are presented in Table 3. From this analysis, the lncRNAs CRNDE (target DEGs: COL4A2, COL6A2, COL6A1, COL5A1, AGRN, POSTN and SGCG) and LINC00152 (target DEG: CDKN1A) stood out. We also

A

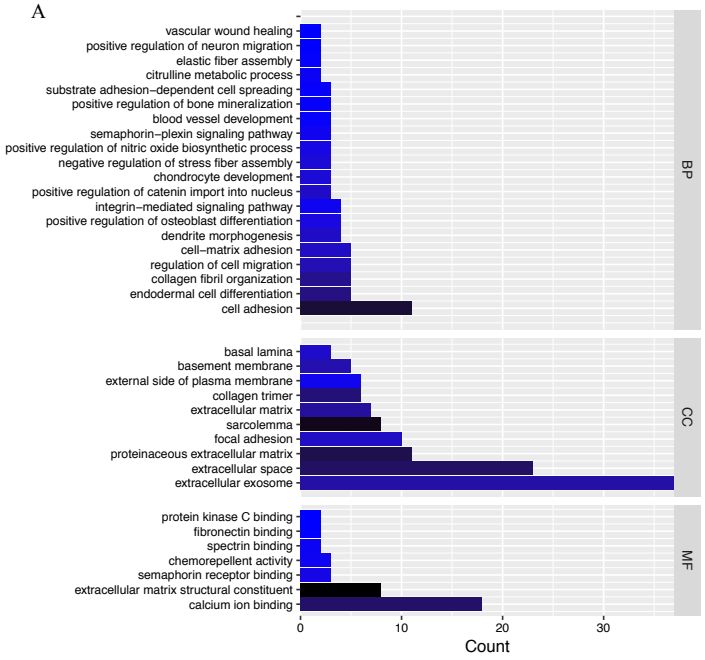

B

Term	Count	PValue	Genes
cell adhesion	11	1.62E-06	NCAM1, TNFAIP6, LAMA4, CD34, MPDZ, TGFBI, COL15A1, VCAN, POSTN, COL5A1, THBS3
endodermal cell differentiation	5	1.08E-04	COL4A2, COL6A1, COL12A1, ITGB2, LAMB1
collagen fibril organization	5	1.97E-04	SFRP2, COL3A1, LOX, COL5A1, DPT
regulation of cell migration	5	1.29E-03	PLXNC1, LAMA4, LMNA, UNC5C, NEXN
cell-matrix adhesion	5	2.81E-03	CD34, COL3A1, ITGB2, NID1, ADAMTS12
dendrite morphogenesis	4	3.39E-03	MAP2, SEMA3A, ITGB1, DCLK1
positive regulation of osteoblast differentiation	4	1.13E-02	CTHRC1, SFRP2, IGF1, BMPR1B
integrin-mediated signaling pathway	4	2.60E-02	PLEK, COL3A1, ITGB2, ITGB1
positive regulation of catenin import into nucleus	3	3.51E-03	DACT1, SULF2, SFRP2
chondrocyte development	3	7.40E-03	SULF2, SFRP2, BMPR1B
negative regulation of stress fiber assembly	3	7.40E-03	DLC1, ARHGAP28, PHLDB2
positive regulation of nitric oxide biosynthetic process	3	1.40E-02	ASS1, PKD2, DDAH2
semaphorin-plexin signaling pathway	3	2.44E-02	SEMA6A, SEMA3C, SEMA3A
blood vessel development	3	3.69E-02	LAMA4, ANTXR1, COL5A1
positive regulation of bone mineralization	3	3.92E-02	SLC8A1, GPM6B, BMPR1B
substrate adhesion-dependent cell spreading	3	4.15E-02	ANTXR1, LAMC1, LAMB1
citrulline metabolic process	2	3.01E-02	ASS1, DDAH2
elastic fiber assembly	2	4.00E-02	FBLN5, LOX
positive regulation of neuron migration	2	4.97E-02	SEMA6A, SEMA3A
vascular wound healing	2	4.97E-02	CD34, MCAM
extracellular exosome	37	6.70E-04	TPPP3, ASS1, NCS1, ITGB2, LRRC15, ITGB1, GPC4, FAT4, TGFBI, PKD2, COL12A1, COL6A1, SEMA3C, ANGPTL1, AGRN, DDAH2, LAMB1, PLEC, DPT, MEST, COL4A2, ACTA2, FBN1, FSCN1, COL15A1, NCKAP1L, NID1, COL5A1, CDH13, COL14A1, FBLN5, RAB15, PAPPA2, ANTXR1, LAMC1, IGFBP3, DNM1
extracellular space	23	2.01E-05	PLAT, CTHRC1, ACTA2, COL3A1, FBN1, COL15A1, IGF1, LRRC17, POSTN, CDH13, COL14A1, SFRP2, FBLN5, TGFBI, SEMA3C, CPA3, COL12A1, VCAN, ANGPTL1, SEMA3A, LAMB1, IGFBP3, DPT
proteinaceous extracellular matrix	11	5.41E-06	GPC4, COL3A1, FBN1, TGFBI, COL15A1, COL6A1, VCAN, POSTN, LOX, ADAMTS12, COL5A1
focal adhesion	10	2.84E-03	DLC1, CDH13, MPZL1, ENAH, MCAM, NEXN, CSRP2, PHLDB2, ITGB1, PLEC
sarcolemma	8	2.52E-07	SLC8A1, SGCG, ANK3, DMD, COL6A1, ITGB1, SGCA, PLEC
extracellular matrix	7	4.58E-04	COL14A1, SFRP2, FBN1, COL15A1, COL12A1, LOXL1, DPT
collagen trimer	6	6.04E-05	COL4A2, COL4A1, C1QTNF3, COL3A1, COL15A1, LOX
external side of plasma membrane	6	2.22E-02	GPC4, CDH13, CD34, MCAM, IL7R, ITGB1
basement membrane	5	1.06E-03	MATN2, FBN1, COL15A1, LAMC1, COL5A1
basal lamina	3	4.29E-03	LAMA4, NID1, AGRN
calcium ion binding	18	2.83E-05	MATN2, SLC8A1, FBN1, PAMR1, NCS1, S100A10, NID1, MCTP1, CDH13, SULF2, FAT4, FBLN5, PKD2, VCAN, AGRN, PLCB2, SGCA, THBS3
extracellular matrix structural constituent	8	7.46E-08	COL4A2, COL4A1, COL3A1, FBN1, VCAN, LAMC1, LAMB1, COL5A1
semaphorin receptor binding	3	1.56E-02	SEMA6A, SEMA3C, SEMA3A
chemorepellent activity	3	2.64E-02	SEMA6A, SEMA3C, SEMA3A
spectrin binding	2	3.02E-02	ANK2, ANK3
fibronectin binding	2	4.98E-02	SFRP2, IGFBP3
protein kinase C binding	2	4.98E-02	DACT1, PLEK

C

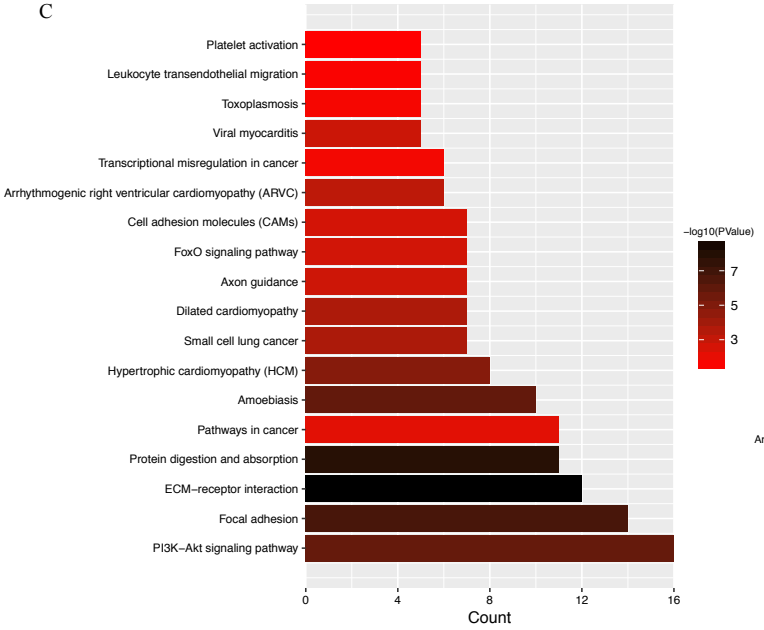

D

Term	Count	PValue	Genes
PI3K-Akt signaling pathway	16	1.56E-06	PIK3CG, COL4A2, COL4A1, COL3A1, IGF1, IL7R, ITGB1, COL5A1, LAMA4, CDKN1A, COL6A2, COL6A1, LAMC1, PRKAA2, LAMB1, THBS3
Focal adhesion	14	1.76E-07	PIK3CG, COL4A2, COL4A1, COL3A1, IGF1, ITGB1, COL5A1, LAMA4, ARHGAP5, COL6A2, COL6A1, LAMC1, LAMB1, THBS3
ECM-receptor interaction	12	1.17E-09	COL4A2, LAMA4, COL4A1, COL3A1, COL6A2, COL6A1, LAMC1, AGRN, LAMB1, ITGB1, COL5A1, THBS3
Protein digestion and absorption	11	1.29E-08	COL4A2, SLC8A1, COL4A1, COL14A1, COL3A1, COL6A2, COL15A1, CPA3, COL6A1, COL12A1, COL5A1
Pathways in cancer	11	7.20E-03	PIK3CG, AGTR1, COL4A2, LAMA4, CDKN1A, COL4A1, IGF1, LAMC1, LAMB1, ITGB1, PLCB2
Amoebiasis	10	1.37E-06	PIK3CG, COL4A2, LAMA4, COL4A1, COL3A1, ITGB2, LAMC1, LAMB1, PLCB2, COL5A1
Hypertrophic cardiomyopathy (HCM)	8	1.67E-05	SGCG, DMD, LMNA, IGF1, PRKAA2, ITGB1, SGCA, SGCB
Small cell lung cancer	7	2.18E-04	PIK3CG, COL4A2, LAMA4, COL4A1, LAMC1, LAMB1, ITGB1
Dilated cardiomyopathy	7	2.33E-04	SGCG, DMD, LMNA, IGF1, ITGB1, SGCA, SGCB
Axon guidance	7	1.84E-03	SEMA6A, PLXNC1, SEMA3C, UNC5C, SEMA3A, ITGB1, EPHA3
FoxO signaling pathway	7	2.43E-03	PIK3CG, CDKN1A, IGF1, BCL6, PRKAA2, IL7R, HOMER1
Cell adhesion molecules (CAMs)	7	2.83E-03	NCAM1, MPZL1, CD34, ITGB2, VCAN, SELPLG, ITGB1
Arrhythmogenic right ventricular cardiomyopathy	6	6.50E-04	SGCG, DMD, LMNA, ITGB1, SGCA, SGCB
Transcriptional misregulation in cancer	6	2.15E-02	PLAT, EYA1, CDKN1A, IGF1, BCL6, IGFBP3
Viral myocarditis	5	1.67E-03	SGCG, DMD, ITGB2, SGCA, SGCB
Toxoplasmosis	5	2.58E-02	LAMA4, IL10RA, LAMC1, LAMB1, ITGB1
Leukocyte transendothelial migration	5	3.33E-02	PIK3CG, ARHGAP5, NCF4, ITGB2, ITGB1
Platelet activation	5	4.42E-02	PIK3CG, COL3A1, ITGB1, PLCB2, COL5A1

Figure 4 **GO functional classification and KEGG pathways enrichment in DEGs.** (A) Histogram of Gene Ontology (GO) functional classification of DEGs. The x-axis represents the number of DEGs, with individual GO terms plotted on the y-axis. All GO terms were grouped into three categories: biological processes, cellular components, and molecular functions. The graph displays only significantly enriched GO terms ($P < 0.05$), with darker blue indicating greater significance. (B) Top BP, CC, and MF terms and their corresponding genes in GO functional enrichment analyses. (C) Histogram of Kyoto Encyclopedia of Genes and Genomes (KEGG) pathways enrichment in DEGs. The x-axis represents the number of DEGs annotated in a pathway, with individual KEGG terms shown on the y-axis. The graph displays only significantly enriched KEGG terms ($P < 0.05$), with darker red indicating greater significance. (D) Individual KEGG terms are shown for each group.

Full-size DOI: 10.7717/peerj.7024/fig-4

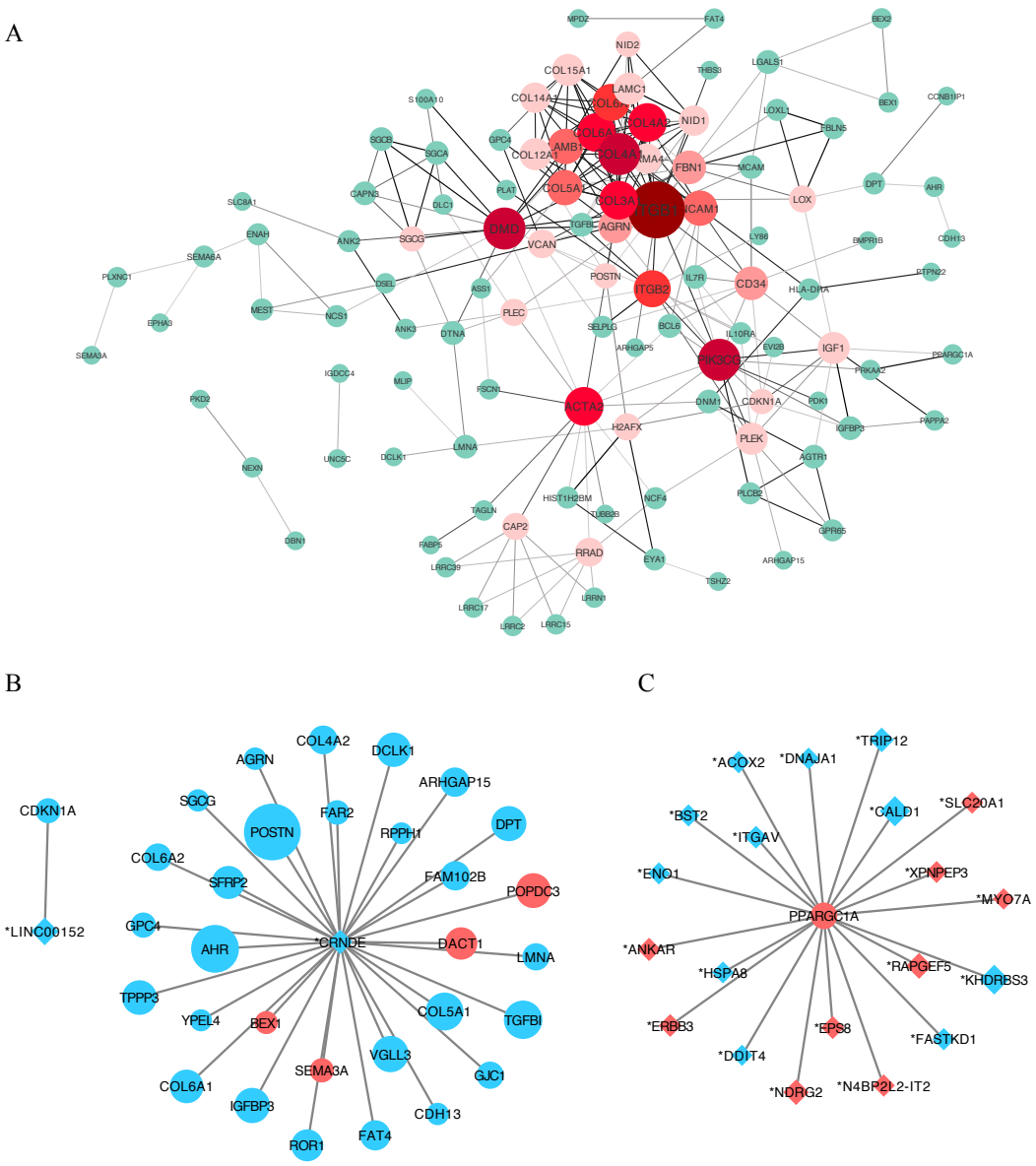

Figure 5 **Protein–protein interaction (PPI) network construction.** (A) A PPI network was used to screen for lncRNA-targeted DEGs. Genes marked in red represent hub genes with a degree of interaction ≥ 5. The darker the connection line, the greater the confidence score. A total of 34 DEGs were identified as age-related hub genes. (B) lncRNA-mRNA association network. Circles indicate mRNAs, with diamonds used to indicate non-protein-coding RNAs. A larger node indicates a larger log_2FC value. Upregulated genes are shown in red and downregulated genes are shown in blue. Here we identified two hub-lncRNAs, CRNDE and LINC00152 and constructed their lncRNA-mRNA networks in graph B. (C) PPARGC1A-lncRNA network. PPARGC1A was a novel DEG which exhibits a close relationship with differently identified age-related lncRNAs.

Full-size DOI: 10.7717/peerj.7024/fig-5

identified an important hub gene, PPARGC1A, which exhibited tight connections with other lncRNAs (Fig. 5C).

Table 2 Hub-genes identified by centiscape (degree ≥ 5) among 174 DEGs.

Name	logFC	AveExpr	P.Value	Transcript_id	Degree
ITGB1	−1.75	16.20	5.68E−04	NM_002211	24
COL4A1	−2.08	6.32	1.06E−05	NM_001845	15
DMD	−2.54	5.21	1.16E−04	NM_000109	15
PIK3CG	−2.76	5.00	2.46E−03	NM_002649	15
ACTA2	−3.98	8.71	2.63E−05	NM_001141945	13
COL3A1	−2.17	14.51	9.08E−03	NM_000090	13
COL4A2	−2.39	5.86	1.27E−06	NM_001846	13
COL6A2	−2.16	7.79	5.55E−03	NM_001849	13
COL6A1	−3.24	12.98	2.16E−03	NM_001848	12
ITGB2	−1.57	5.28	2.96E−02	NM_000211	12
COL5A1	−3.98	12.58	4.02E−03	NM_000093	11
LAMB1	−4.11	7.02	6.24E−05	NM_002291	11
NCAM1	−2.70	9.34	8.57E−03	NM_000615	11
AGRN	−1.29	5.82	3.74E−05	NM_198576	10
CD34	−2.22	8.14	8.45E−03	NM_001025109	10
FBN1	−2.32	12.40	2.56E−05	NM_000138	10
COL12A1	−2.64	14.08	4.18E−05	NM_004370	9
COL15A1	−3.08	8.66	7.14E−03	NM_001855	9
IGF1	−2.17	8.53	2.33E−04	NM_000618	9
LAMC1	−1.14	5.81	4.06E−03	NM_002293	9
PLEK	−3.59	7.30	2.46E−04	NM_002664	9
COL14A1	−4.13	12.30	7.96E−04	NM_021110	8
LAMA4	−1.82	7.39	8.45E−05	NM_001105206	8
NID1	−4.19	9.38	2.22E−08	NM_002508	8
RRAD	−1.19	4.96	3.31E−03	NM_001128850	7
VCAN	−4.09	10.96	2.68E−04	NM_001126336	7
CAP2	−1.17	6.67	2.07E−03	NM_006366	6
H2AFX	−1.19	6.96	2.48E−04	NM_002105	6
LOX	−2.88	11.46	1.92E−03	NM_001178102	6
PLEC	−1.05	8.23	4.22E−03	NM_000445	6
CDKN1A	−1.73	7.04	6.11E−03	NM_000389	5
NID2	−3.56	9.41	3.20E−05	NM_007361	5
POSTN	−7.29	10.68	1.97E−03	NM_001135934	5
SGCG	−1.26	4.39	3.62E−02	NM_000231	5

qRT-PCR validation

To confirm the results of our bioinformatic analysis, we examined the expression of CRNDE and LNC00152 by qRT-PCR in 16 cartilage samples. According to Fig. 6, the transcriptional levels of CRNDE and LNC00152 were significantly decreased in OA group compared with the normal group. These results were consistent with our previous integrative analysis listed in Table 3 and showed the same trends of these hub lncRNAs.

Table 3 All differentially expressed lncRNAs upstream of DEGs.

Gene symbol	logFC	AveExpr	P.Value	change
ACOX2	−1.29	5.88	1.83E–05	DOWN
ANKAR	1.44	9.79	6.63E–05	UP
BST2	−1.26	6.01	8.68E–04	DOWN
CALD1	−2.03	11.76	8.24E–05	DOWN
CRNDE	−1.62	6.96	5.43E–06	DOWN
DDIT4	−1.08	6.48	6.00E–03	DOWN
DNAJA1	−1.18	10.99	1.41E–04	DOWN
ENO1	−1.24	12.23	3.24E–02	DOWN
EPS8	1.39	10.73	2.24E–04	UP
ERBB3	1.35	6.31	1.90E–03	UP
FASTKD1	−1.27	10.04	2.31E–03	DOWN
HSPA8	−1.20	14.94	7.94E–05	DOWN
ITGAV	−1.35	9.69	6.15E–04	DOWN
KHDRBS3	−2.58	7.15	4.01E–04	DOWN
LINC00152	−2.20	8.75	2.19E–04	DOWN
MYO7A	1.09	6.56	4.67E–03	UP
N4BP2L2-IT2	1.27	11.17	1.64E–04	UP
NDRG2	1.83	9.05	9.92E–03	UP
RAPGEF5	1.88	5.55	2.01E–05	UP
SLC20A1	1.23	11.19	1.77E–02	UP
TMEM161B-AS1	1.02	7.91	1.70E–05	UP
TRIP12	−1.67	10.53	1.84E–04	DOWN
XPNPEP3	1.22	7.23	1.04E–03	UP

DISCUSSION

LncRNAs have emerged as critical modulators of transcriptional, post-transcriptional, and epigenetic gene regulation, with emerging evidence suggesting a relationship between lncRNAs and OA. With the development of high-throughput sequencing technology, an increasing number of RNA-sequencing projects have been performed, identifying key functional mRNAs, miRNAs, lncRNAs, and circRNAs in the development of OA. *Xing et al. (2014)* reported six lncRNAs, including HOTAIR, GAS5, PMS2L2, RP11–445H22.4, H19, and CTD-2574D22.4, which were differently expressed in OA samples in microarray analyses (*Xing et al., 2014*). Subsequent studies have since described lncRNAs expression patterns in human osteoarthritic cartilage using a combination of DNA microarray and bioinformatic analyses (*Fu et al., 2015*). Additional lncRNAs including PACER, CILinc01, and CILinc02, have also been reported in human hip OA chondrocytes, and were significantly associated with the OA inflammatory response (*Pearson et al., 2016*). Similarly, when comparing the expression of lncRNAs in OA cartilage of variable severity, four hub lncRNAs, SNHG5, ZFAS1, GAS5, and DANCR, were identified as key functional mediators in OA pathogenesis (*Xiao et al., 2018*).

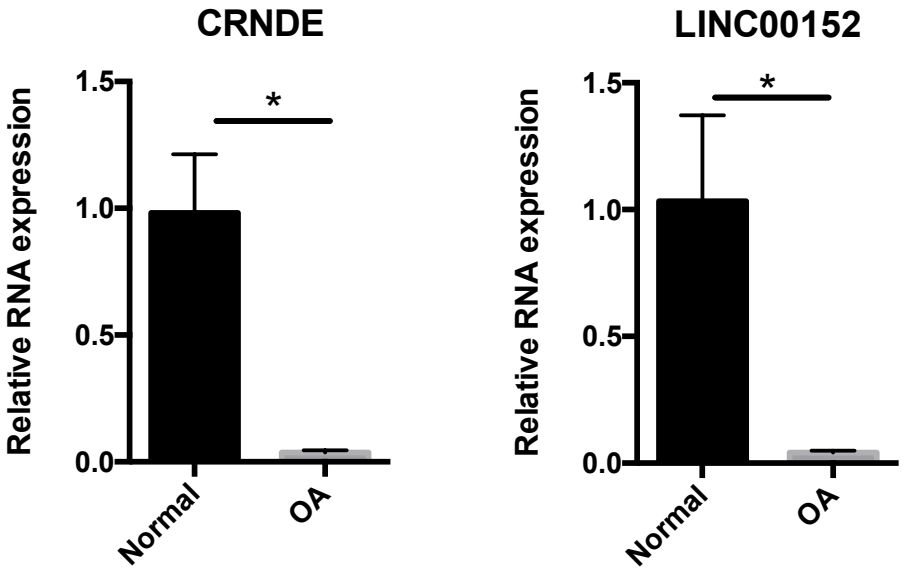

Figure 6 Relative expression of CRNDE (A) and LINC00152 (B) in human samples. Relative expression of CRNDE (A) and LINC00152 (B) in human samples, as determined by RT-PCR. Each column represents the mean ± SD. The OA group exhibited lower-level expression of CRNDE and LINC00152 compared with the normal group. OA samples were obtained from eight osteoarthritis patients who underwent total hip arthroplasty. Normal samples were obtained from eight femoral neck fracture patients who underwent total hip arthroplasty. $^{*}p < 0.05$ vs. normal group.

Full-size DOI: 10.7717/peerj.7024/fig-6

Although many bioinformatics analyses have revealed differences in gene expression patterns in OA samples, few have examined what, if any, age-related lncRNAs are involved in this process. Therefore, a detailed database of lncRNA observed in rat knee articular cartilage at different developmental stages was used in our study. By comparing differential gene expression in five stages, newborn (T0), youth (T1), adult (T2), early-stage elderly (T3), and later-stage elderly (T4), a set of age-related DEGs were identified. Next, we identified the homologous human genes for each of our age-related rat DEGs, which then were compared against a separate set of DEGs extracted from a human OA lncRNAs expression database. Our results broadly confirmed dysregulated gene in age-related cartilage, including ITGB1, COL4A1, DMD, PIK3CG, ACTA2, COL3A1, COL4A2, COL6A2, and COL6A1. We also identified two hub lncRNAs, CRNDE and LINC00152, which were not identified in previous studies.

LINC00152 is an 828 bp lncRNA located on chromosome 2p11.2. Previous studies have found that LINC00152 plays an oncogenic role in the development of a wide range of tumor types (*Chen et al., 2018a*; *Chen et al., 2018c*). Enhanced LINC00152 expression has also been found to be a potential prognostic biomarker in patients with lung and colorectal cancers (*Chen et al., 2018b*; *Li et al., 2017b*). LINC00152 also acts as a sponge for various miRNAs, as shown in a recent report describing the interaction between LINC00152 and miR-139 in colorectal cancer cells (*Bian et al., 2017*). This observation is important, as emerging evidence has shown increased expression of miR-139 in OA cartilage, with increased miR-139 expression resulting in higher expression of IL-6 and chondrocyte apoptosis (*Hu*

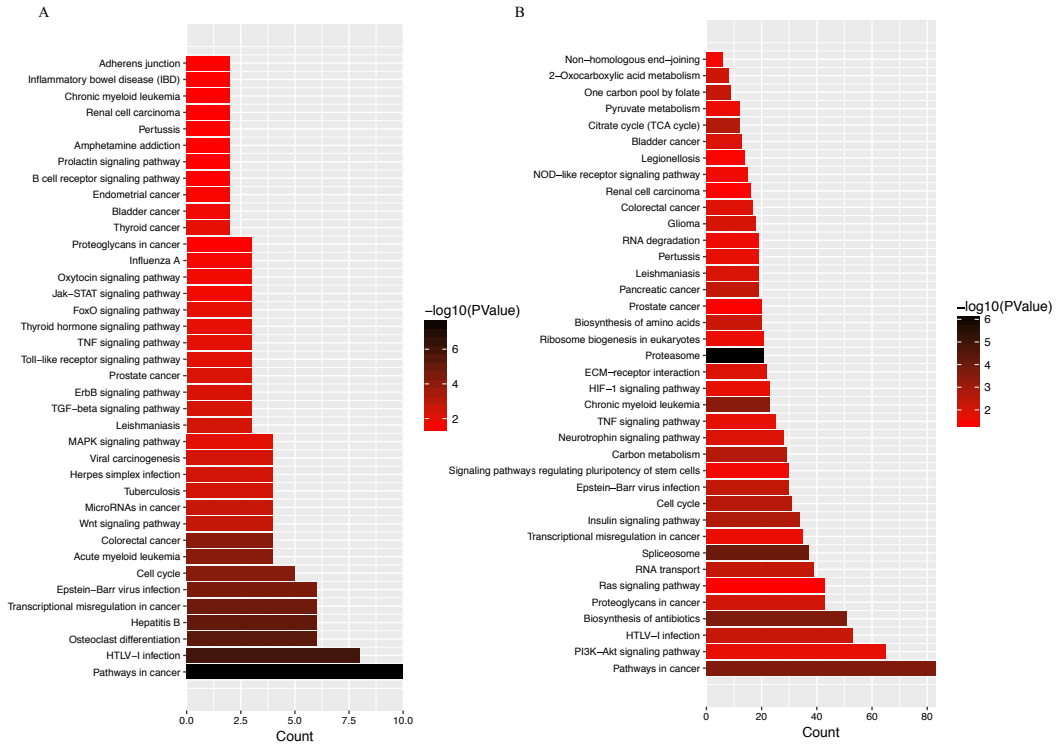

Figure 7 **KEGG analyses of (A) LINC00152 and (B) CRNDE.** The x-axis represents the number of predicted target gene, with individual KEGG terms shown on the y-axis.

Full-size DOI: 10.7717/peerj.7024/fig-7

et al., 2016; *Makki & Haqqi, 2015*). Furthermore, KEGG analyses of LINC00152 (Fig. 7A) revealed strong associations between osteoclast differentiation, cell cycle, and Wnt signaling pathways and LINC00152 in OA. Given these observations, the LINC00152/miRNA axis will likely become a major focus of future OA studies.

Another hub lncRNA identified in our study, CRNDE, is a 1910 nt cancer-secreted lncRNA transcribed by human chromosome 16 (16q12.2). This lncRNA has been observed in a variety of cancers, including osteosarcoma, colorectal, cervical, and gastric cancers (*Ding et al., 2017*; *Hu et al., 2017*; *Li et al., 2018*; *Meng et al., 2017*). *Huan et al. (2017)* reported an important role for CRNDE in the pathophysiology of human breast cancer. CRNDE was shown to modulate the Wnt/β-catenin signaling pathway by repressing miR-136 expression via the miRNA sponge mechanism, resulting in significant difference in proliferation, migration, and invasion of breast cancer cells. Coincidentally, another group demonstrated that miR-136 plays an important role in the regulation of chondrogenesis in human adipose-derived stem cells (*Zhang et al., 2012*). Further research revealed that miR-136 bound to the 3′-UTR of MMP13, a key catabolic enzyme involved in the degradation of ECM (*Li et al., 2017a*). By competitively binding with miR-136, circRNA-CER regulates MMP13 expression, further promoting chondrocyte ECM degradation (*Liu et al., 2016*). Beyond miR136, decades of research have shown that CRNDE modulates miR-384 activity in a number of tumor cell types (*Chen et al., 2016*; *Zheng et al., 2016*). Recently, miR-384–5p

Table 4 Potential functional miRNAs associated with hub lncRNAs.

predicted miRNAs for LINC00152	predicted miRNAs for CRNDE
hsa-miR-106a-5p	hsa-miR-136-5p
hsa-miR-125a-3p	hsa-miR-384
hsa-miR-129-5p	hsa-miR-145-5p
hsa-miR-136-5p	
hsa-miR-1-3p	
hsa-miR-149-5p	
hsa-miR-185-5p	
hsa-miR-193a-3p	
hsa-miR-193b-3p	
hsa-miR-206	
hsa-miR-24-3p	
hsa-miR-320a	
hsa-miR-320b	
hsa-miR-320c	
hsa-miR-320d	
hsa-miR-376a-3p	
hsa-miR-376b-3p	
hsa-miR-376c-3p	
hsa-miR-383-5p	
hsa-miR-485-5p	
hsa-miR-503-5p	
hsa-miR-613	
hsa-miR-873-5p	

was shown to induce OA by regulating the expression of SOX9 and downregulating activity of the NF-κB signaling pathway (*Zhang et al., 2018*). Taken together, these data suggest that CRNDE can act as a miRNA sponge, competing for miRNA binding with protein-coding transcripts, although the exact mechanism of lncRNA CRNDE-mediated regulation of OA pathogenesis remains to be investigated. Other potential miRNAs related to these two hub lncRNAs have been curated from databases (RAID 2.0, starBASE v2.0, miRTarBase), and are listed in Table 4. Targets suggested by KEGG analyses suggest that the PI3K–Akt signaling pathway, proteoglycan metabolism, and the Ras signaling pathway are promising targets (Fig. 7B).

Outside of lncRNAs, the PPI network identified PPARGC1A as a novel mediator of OA pathogenesis due to its close relationship with various age-related lncRNAs. PPARGC1A, also known as human-accelerated region 20, encodes the peroxisome proliferator-activated receptor gamma coactivator 1-alpha (PGC-1α). PGC-1 α is widely viewed as a master regulator of mitochondrial biogenesis (*Liang & Ward, 2006*). Reduced expression of PGC-1α has been observed in knee cartilage of aged mice, where it may attenuate oxidative stress and cartilage erosion in OA (*Zhao et al., 2014*). Activation of PGC-1α expression significantly enhances mitochondrial biogenesis and inhibits oxidative phosphorylation in

OA chondrocytes. Similarly, the AMP-activated protein kinase/PGC-1 signaling pathway is an effective target for OA treatment in a rat model (*Wang et al., 2018a*).

CONCLUSIONS

The current study identified a series of DEGs and lncRNAs in each developmental stage of articular cartilage. Using a series of bioinformatics analyses, two pivotal lncRNAs, CRNDE and LINC00152, were identified, which are strongly associated with age-related cartilage degradation. Further functional analyses suggest a potential mechanism through which these hub lncRNAs mediate OA pathogenesis. Our results highlight the important role of lncRNAs in the pathogenesis of OA, although more research is necessary to confirm our findings.

ACKNOWLEDGEMENTS

We are grateful to GEO database and its contributors who provided their data for this analysis.

ADDITIONAL INFORMATION AND DECLARATIONS

Funding

This study was supported by the National Natural Science Foundation of China (No. 81301584). The funders had no role in study design, data collection and analysis, decision to publish, or preparation of the manuscript.

Grant Disclosures

The following grant information was disclosed by the authors:
National Natural Science Foundation of China: No. 81301584.

Competing Interests

The authors declare there are no competing interests.

Author Contributions

- Pengfei Hu, Fangfang Sun performed the experiments, analyzed the data, contributed reagents/materials/analysis tools, prepared figures and/or tables, authored or reviewed drafts of the paper, approved the final draft.
- Jisheng Ran performed the experiments, authored or reviewed drafts of the paper.
- Lidong Wu conceived and designed the experiments, approved the final draft.

Human Ethics

The following information was supplied relating to ethical approvals (i.e., approving body and any reference numbers):

This study was approved by the Ethics Committee of the 2nd Affiliated Hospital, School of medicine, Zhejiang University, Hangzhou, China.

Data Availability

The following information was supplied regarding data availability:

Data is available in the GEO database, accession numbers: GSE66554 and GSE113825.

Supplemental Information

Supplemental information for this article can be found online at http://dx.doi.org/10.7717/peerj.7024#supplemental-information.

REFERENCES

Ashburner M, Ball CA, Blake JA, Botstein D, Butler H, Cherry JM, Davis AP, Dolinski K, Dwight SS, Eppig JT, Harris MA, Hill DP, Issel-Tarver L, Kasarskis A, Lewis S, Matese JC, Richardson JE, Ringwald M, Rubin GM, Sherlock G. 2000. Gene ontology: tool for the unification of biology. The Gene Ontology Consortium. *Nature Genetics* **25**:25–29 DOI 10.1038/75556.

Bian Z, Zhang J, Li M, Feng Y, Yao S, Song M, Qi X, Fei B, Yin Y, Hua D, Huang Z. 2017. Long non-coding RNA LINC00152 promotes cell proliferation, metastasis, and confers 5-FU resistance in colorectal cancer by inhibiting miR-139-5p. *Oncogenesis* **6**:Article 395 DOI 10.1038/s41389-017-0008-4.

Campisi J, d'Addadi Fagagna F. 2007. Cellular senescence: when bad things happen to good cells. *Nature Reviews Molecular Cell Biology* **8**:729–740 DOI 10.1038/nrm2233.

Cao W, Wu W, Shi F, Chen X, Wu L, Yang K, Tian F, Zhu M, Chen G, Wang W, Biddle FG, Gu J. 2013. Integrated analysis of long noncoding RNA and coding RNA expression in esophageal squamous cell carcinoma. *International Journal of Genomics* **2013**:Article 480534.

Chen P, Fang X, Xia B, Zhao Y, Li Q, Wu X. 2018a. Long noncoding RNA LINC00152 promotes cell proliferation through competitively binding endogenous miR-125b with MCL-1 by regulating mitochondrial apoptosis pathways in ovarian cancer. *Cancer Medicine* **7**:4530–4541 DOI 10.1002/cam4.1547.

Chen Z, Cai X, Chang L, Xia Y, Wang L, Hou Y, Li L, Pan D, Li F, Liu S, Xiong W, Li W. 2018b. LINC00152 is a potential biomarker involved in the modulation of biological characteristics of residual colorectal cancer cells following chemoradiotherapy. *Oncology Letters* **15**:4177–4184.

Chen ZP, Wei JC, Wang Q, Yang P, Li WL, He F, Chen HC, Hu H, Zhong JB, Cao J. 2018c. Long noncoding RNA 00152 functions as a competing endogenous RNA to regulate NRP1 expression by sponging with miRNA206 in colorectal cancer. *International Journal of Oncology* **53**:1227–1236.

Chen Z, Yu C, Zhan L, Pan Y, Chen L, Sun C. 2016. LncRNA CRNDE promotes hepatic carcinoma cell proliferation, migration and invasion by suppressing miR-384. *American Journal of Cancer Research* **6**:2299–2309.

Ding C, Cicuttini F, Scott F, Cooley H, Jones G. 2005. Association between age and knee structural change: a cross sectional MRI based study. *Annals of the Rheumatic Diseases* **64**:549–555 DOI 10.1136/ard.2004.023069.

Ding J, Li J, Wang H, Tian Y, Xie M, He X, Ji H, Ma Z, Hui B, Wang K, Ji G. 2017. Long noncoding RNA CRNDE promotes colorectal cancer cell proliferation via epigenetically silencing DUSP5/CDKN1A expression. *Cell Death & Disease* **8**:e2997 DOI 10.1038/cddis.2017.328.

Fu M, Huang G, Zhang Z, Liu J, Zhang Z, Huang Z, Yu B, Meng F. 2015. Expression profile of long noncoding RNAs in cartilage from knee osteoarthritis patients. *Osteoarthritis Cartilage* **23**:423–432 DOI 10.1016/j.joca.2014.12.001.

Ganguly P, El-Jawhari JJ, Giannoudis PV, Burska AN, Ponchel F, Jones EA. 2017. Age-related changes in bone marrow mesenchymal stromal cells: a potential impact on osteoporosis and osteoarthritis development. *Cell Transplantation* **26**:1520–1529 DOI 10.1177/0963689717721201.

Hao Y, Wu W, Shi F, Dalmolin RJ, Yan M, Tian F, Chen X, Chen G, Cao W. 2015. Prediction of long noncoding RNA functions with co-expression network in esophageal squamous cell carcinoma. *BMC Cancer* **15**:168 DOI 10.1186/s12885-015-1179-z.

Henrotin YE, Bruckner P, Pujol JP. 2003. The role of reactive oxygen species in homeostasis and degradation of cartilage. *Osteoarthritis Cartilage* **11**:747–755 DOI 10.1016/S1063-4584(03)00150-X.

Hu CE, Du PZ, Zhang HD, Huang GJ. 2017. Long noncoding RNA CRNDE promotes proliferation of gastric cancer cells by targeting miR-145. *Cellular Physiology and Biochemistry* **42**:13–21 DOI 10.1159/000477107.

Hu J, Wang Z, Shan Y, Pan Y, Ma J, Jia L. 2018. Long non-coding RNA HOTAIR promotes osteoarthritis progression via miR-17-5p/FUT2/beta-catenin axis. *Cell Death & Disease* **9**:Article 711.

Hu W, Zhang W, Li F, Guo F, Chen A. 2016. miR-139 is up-regulated in osteoarthritis and inhibits chondrocyte proliferation and migration possibly via suppressing EIF4G2 and IGF1R. *Biochemical and Biophysical Research Communications* **474**:296–302 DOI 10.1016/j.bbrc.2016.03.164.

Huan J, Xing L, Lin Q, Xui H, Qin X. 2017. Long noncoding RNA CRNDE activates Wnt/beta-catenin signaling pathway through acting as a molecular sponge of microRNA-136 in human breast cancer. *American Journal of Translational Research* **9**:1977–1989.

Huang Y. 2018. The novel regulatory role of lncRNA-miRNA-mRNA axis in cardiovascular diseases. *Journal of Cellular and Molecular Medicine* **22**:5768–5775 DOI 10.1111/jcmm.13866.

Hunter DJ, Felson DT. 2006. Osteoarthritis. *BMJ* **332**:639–642 DOI 10.1136/bmj.332.7542.639.

Kanehisa M, Goto S. 2000. KEGG: kyoto encyclopedia of genes and genomes. *Nucleic Acids Research* **28**:27–30 DOI 10.1093/nar/28.1.27.

Leti F, DiStefano JK. 2017. Long noncoding RNAs as diagnostic and therapeutic targets in type 2 diabetes and related complications. *Genes* **8**:Article 207 DOI 10.3390/genes8080207.

Li H, Wang D, Yuan Y, Min J. 2017a. New insights on the MMP-13 regulatory network in the pathogenesis of early osteoarthritis. *Arthritis Research & Therapy* **19**:Article 248 DOI 10.1186/s13075-017-1454-2.

Li N, Feng XB, Tan Q, Luo P, Jing W, Zhu M, Liang C, Tu J, Ning Y. 2017b. Identification of circulating long noncoding RNA Linc00152 as a novel biomarker for diagnosis and monitoring of non-small-cell lung cancer. *Disease Markers* **2017**:Article 7439698.

Li YF, Li SH, Liu Y, Luo YT. 2017c. Long noncoding RNA CIR promotes chondrocyte extracellular matrix degradation in osteoarthritis by acting as a sponge for Mir-27b. *Cellular Physiology and Biochemistry* **43**:602–610 DOI 10.1159/000480532.

Li Z, Tang Y, Xing W, Dong W, Wang Z. 2018. LncRNA, CRNDE promotes osteosarcoma cell proliferation, invasion and migration by regulating Notch1 signaling and epithelial-mesenchymal transition. *Experimental and Molecular Pathology* **104**:19–25 DOI 10.1016/j.yexmp.2017.12.002.

Liang H, Ward WF. 2006. PGC-1alpha: a key regulator of energy metabolism. *Advances in Physiology Education* **30**:145–151 DOI 10.1152/advan.00052.2006.

Liu Q, Zhang X, Hu X, Dai L, Fu X, Zhang J, Ao Y. 2016. Circular RNA related to the chondrocyte ECM regulates MMP13 expression by functioning as a MiR-136 'Sponge' in human cartilage degradation. *Scientific Reports* **6**:22572 DOI 10.1038/srep22572.

Loeser RF. 2017. The role of aging in the development of osteoarthritis. *Transactions of the American Clinical and Climatological Association* **128**:44–54.

Makki MS, Haqqi TM. 2015. miR-139 modulates MCPIP1/IL-6 expression and induces apoptosis in human OA chondrocytes. *Experimental & Molecular Medicine* **47**:e189 DOI 10.1038/emm.2015.66.

Meng Y, Li Q, Li L, Ma R. 2017. The long non-coding RNA CRNDE promotes cervical cancer cell growth and metastasis. *Biological Chemistry* **399**:93–100.

Pearson MJ, Philp AM, Heward JA, Roux BT, Walsh DA, Davis ET, Lindsay MA, Jones SW. 2016. Long intergenic noncoding rnas mediate the human chondrocyte inflammatory response and are differentially expressed in osteoarthritis cartilage. *Arthritis & Rheumatology* **68**:845–856.

Ponting CP, Oliver PL, Reik W. 2009. Evolution and functions of long noncoding RNAs. *Cell* **136(4)**:629–641 DOI 10.1016/j.cell.2009.02.006.

Ritchie ME, Phipson B, Wu D, Hu Y, Law CW, Shi W, Smyth GK. 2015. limma powers differential expression analyses for RNA-sequencing and microarray studies. *Nucleic Acids Research* **43(7)**:e47 DOI 10.1093/nar/gkv007.

Shane Anderson A, Loeser RF. 2010. Why is osteoarthritis an age-related disease? *Best Practice & Research Clinical Rheumatology* **24**:15–26 DOI 10.1016/j.berh.2009.08.006.

Silverwood V, Blagojevic-Bucknall M, Jinks C, Jordan JL, Protheroe J, Jordan KP. 2015. Current evidence on risk factors for knee osteoarthritis in older adults: a systematic review and meta-analysis. *Osteoarthritis Cartilage* **23**:507–515 DOI 10.1016/j.joca.2014.11.019.

Szklarczyk D, Franceschini A, Wyder S, Forslund K, Heller D, Huerta-Cepas J, Simonovic M, Roth A, Santos A, Tsafou KP, Kuhn M, Bork P, Jensen LJ, Von Mering C. 2015. STRING v10: protein-protein interaction networks, integrated over the tree of life. *Nucleic Acids Research* **43(D1)**:D447–D452 DOI 10.1093/nar/gku1003.

Tang X, Wang S, Zhan S, Niu J, Tao K, Zhang Y, Lin J. 2016. The prevalence of symptomatic knee osteoarthritis in China: results from the China health and retirement longitudinal study. *Arthritis & Rheumatology* **68**:648–653 DOI 10.1002/art.39465.

Wang L, Shan H, Wang B, Wang N, Zhou Z, Pan C, Wang F. 2018a. Puerarin attenuates osteoarthritis via upregulating AMP-activated protein kinase/proliferator-activated receptor-gamma coactivator-1 signaling pathway in osteoarthritis rats. *Pharmacology* **102**:117–125 DOI 10.1159/000490418.

Wang Y, Luo TB, Liu L, Cui ZQ. 2018b. LncRNA LINC00311 promotes the proliferation and differentiation of osteoclasts in osteoporotic rats through the notch signaling pathway by targeting DLL3. *Cellular Physiology and Biochemistry* **47**:2291–2306 DOI 10.1159/000491539.

Wu W, Billinghurst RC, Pidoux I, Antoniou J, Zukor D, Tanzer M, Poole AR. 2002. Sites of collagenase cleavage and denaturation of type II collagen in aging and osteoarthritic articular cartilage and their relationship to the distribution of matrix metalloproteinase 1 and matrix metalloproteinase 13. *Arthtitis and Rheumatism* **46**:2087–2094 DOI 10.1002/art.10428.

Xiang S, Li Z, Bian Y, Weng X. 2018. Identification of changed expression of mRNAs and lncRNAs in osteoarthritic synovium by RNA-sequencing. *Gene* **685**:55–61 DOI 10.1016/j.gene.2018.10.076.

Xiao K, Yang Y, Bian Y, Feng B, Li Z, Wu Z, Qiu G, Weng X. 2018. Identification of differentially expressed long noncoding RNAs in human knee osteoarthritis. *Journal of Cellular Biochemistry* **120**:4620–4633 DOI 10.1002/jcb.27750.

Xing D, Liang JQ, Li Y, Lu J, Jia HB, Xu LY, Ma XL. 2014. Identification of long noncoding RNA associated with osteoarthritis in humans. *Orthopaedic Surgery* **6**:288–293 DOI 10.1111/os.12147.

Ye D, Jian W, Feng J, Liao X. 2018. Role of long noncoding RNA ZFAS1 in proliferation, apoptosis and migration of chondrocytes in osteoarthritis. *Biomedicine and Pharmacotherapy* **104**:825–831 DOI 10.1016/j.biopha.2018.04.124.

Zhang W, Cheng P, Hu W, Yin W, Guo F, Chen A, Huang H. 2018. Inhibition of microRNA-384-5p alleviates osteoarthritis through its effects on inhibiting apoptosis of cartilage cells via the NF-kappaB signaling pathway by targeting SOX9. *Cancer Gene Therapy* **25**:326–338 DOI 10.1038/s41417-018-0029-y.

Zhang Z, Kang Y, Zhang Z, Zhang H, Duan X, Liu J, Li X, Liao W. 2012. Expression of microRNAs during chondrogenesis of human adipose-derived stem cells. *Osteoarthritis Cartilage* **20**:1638–1646 DOI 10.1016/j.joca.2012.08.024.

Zhao X, Petursson F, Viollet B, Lotz M, Terkeltaub R, Liu-Bryan R. 2014. Peroxisome proliferator-activated receptor gamma coactivator 1alpha and FoxO3A mediate chondroprotection by AMP-activated protein kinase. *Arthritis & Rheumatology* **66**:3073–3082 DOI 10.1002/art.38791.

Zheng J, Liu X, Wang P, Xue Y, Ma J, Qu C, Liu Y. 2016. CRNDE promotes malignant progression of glioma by attenuating miR-384/PIWIL4/STAT3 Axis. *Molecular Therapy* **24**:1199–1215 DOI 10.1038/mt.2016.71.